

One-Shot Multi-Rate Pruning of Graph Convolutional Networks

Hichem Sahbi

Sorbonne University, CNRS, LIP6, F-75005, Paris, France

◆

Abstract

In this paper, we devise a novel lightweight Graph Convolutional Network (GCN) design dubbed as Multi-Rate Magnitude Pruning (MRMP) that jointly trains network topology and weights. Our method is variational and proceeds by aligning the weight distribution of the learned networks with an a priori distribution. In the one hand, this allows implementing any fixed pruning rate, and also enhancing the generalization performances of the designed lightweight GCNs. In the other hand, MRMP achieves a joint training of multiple GCNs, on top of shared weights, in order to extrapolate accurate networks at any targeted pruning rate without retraining their weights. Extensive experiments conducted on the challenging task of skeleton-based recognition show a substantial gain of our lightweight GCNs particularly at very high pruning regimes.

1 INTRODUCTION

With the re-emergence of deep neural networks [63], many computer vision tasks have been successfully revisited [29], [30], [50], [52], [110], [145]. These tasks have been handled with more and more accurate but *oversized* networks, and this makes their deployment on edge devices very challenging. Particularly, in hand-gesture recognition and human computer interaction, edge devices are endowed with limited computational resources. Therefore, fast and lightweight models with high recognition performances are vital for skeleton-based recognition. Recent learning models applying deep networks have shown saturated recognition accuracy without substantial improvement, while computational efficiency still remains a serious issue. Among these learning models, graph convolutional networks (GCNs) are known to be effective particularly on non-euclidean domains such as skeleton data [148], [149]. At least two categories of GCNs are known in the literature; spatial and spectral. Spectral methods first map graph signals from the input to the Fourier domain prior to achieve convolution, and then map back the convolved signals in the input domain [3], [11], [13], [35], [58], [69], [74], [94], [114]. Spatial methods proceed by aggregating node signals using multi-head attention (MHA) before applying convolutions on the resulting node aggregates [21], [23], [60], [96], [104], [107], [133], [134]. Spatial GCNs are known to be more effective compared to spectral ones, however, their main downside resides in their computational complexity. Hence, a major problem is how to make these networks lightweight while maintaining their high accuracy [4], [32], [33], [40], [43], [112], [117], [118], [130].

Many existing works consider the challenge of lightweight network design such as tensor decomposition [39], quantization [24], distillation [1], [36], [97], [142], [147] and pruning [26], [27], [64], [126]. Pruning methods, in particular, are highly effective, and their principle is to remove connections whose impact on the classification performances is the least important. Two major categories of pruning approaches exist in the sota; structured [73], [89] and unstructured [24],

[26]. The former aims at zeroing-out weights of entire filters or channels whilst the latter aims at removing weights separately. While structured methods provide computationally more efficient networks, they are less precise compared to unstructured techniques; indeed, the latter produce more flexible (and hence more accurate) networks which are computationally still efficient. Magnitude pruning (MP) [24] is one of the widely used unstructured methods that proceeds by removing the smallest weight connections before retraining the resulting pruned network. While being able to reach any fixed (targeted) pruning rate, MP is clearly not optimal as it *decouples* the training of network weights from topology. Hence, removed connections cannot be recovered when retraining the pruned networks, and this leads to suboptimal performances. Moreover, the full retraining of the pruned networks (at multiple pruning rates) makes MP highly intractable.

In this paper, we introduce a novel alternative for magnitude pruning referred to as MRMP (Multi-Rate Magnitude Pruning) that allows (i) *coupling* the training of network weights and topology, (ii) *learning simultaneously multiple* network instances for different pruning rates, and (iii) *extrapolating* accurate networks at any unseen pruning rate without retraining. The proposed method constrains the distribution of the learned weights to match a fixed targeted distribution and this allows, *via a band-stop mechanism*, to dropout all the connections up to a given targeted pruning rate. The advantage of the proposed contribution is twofold; in the one hand, it constrains the learned weights to fit a targeted distribution and this leads to better generalization. In the other hand, it allows obtaining fully trained networks at any unseen pruning rate instantaneously without weight retraining.

Considering all the aforementioned issues, the main contributions of our paper include

- A band-stop weight parametrization that achieves a *joint* training of GCN topology and weights (see section 3). This parametrization relies on shared latent weights that reduce the number of training parameters of the pruned GCNs.
- A KLD (Kullback Leibler Divergence) based regularizer that constrains the latent weights to fit an *a priori* distribution, and this allows implementing any targeted pruning rate *almost* exactly (see section 3.1).
- A multiple magnitude pruning that obtains optimal GCNs at any targeted pruning rate thanks to the band-stop parametrization and the KLD regularizer. The latter defines a continuum of *weight aggregates* associated to GCNs with increasing pruning rates. These *weight aggregates* allow generalizing across unseen pruning rates without retraining (see section 3.2).
- Extensive experiments conducted on the challenging task of skeleton-based recognition corroborate all these findings and show the outperformance of our method against the related work (see section 4).

2 RELATED WORK

We review and discuss subsequently the related work in variational pruning and skeleton-based recognition, and the limitations that motivate our contributions.

Variational Pruning. The general recipe of variational pruning consists in learning both weights and binary masks that capture topology of pruned networks. This is achieved by minimizing a loss that combines (via a mixing hyperparameter) a classification error and a regularizer which controls the sparsity of the resulting masks [89], [90], [128]. However, these methods are powerless to implement any given targeted pruning rate (cost) without overtrying multiple settings of the mixing hyperparameters. Alternative methods explicitly model the cost, using ℓ_0 -based criteria

[90], [106], in order to minimize the discrepancy between the observed cost and the targeted one. Nonetheless, the underlying optimization problems are highly combinatorial and existing solutions usually rely on sampling heuristics or relaxation, such as ℓ_1/ℓ_2 -based, entropy, etc. [7], [20], [61], [132]; the latter promote sparsity, but are powerless to implement any given target cost exactly, and also result into overpruning effects leading to disconnected subnetworks, with weak generalization, especially at very high pruning regimes. Besides, most of the existing solutions, including magnitude pruning [24], decouple the training of network topology (masks) from weights, and this makes the learning of pruned networks clearly suboptimal.

Skeleton-based Recognition. With the emergence of sensors, including Intel RealSense [56] and Microsoft Kinect [143], interest in skeleton-based recognition is increasingly growing [6]. Hand-gesture and action recognition are two neighboring tasks which have initially been tackled using RGB [42], [88], [122], [123], [139], depth [103], [124], shape/normals [49], [77], [105], [109], [111], [137], [140], [141] and also skeleton-based techniques [125]. In particular, early skeleton-based methods are based on modeling human motions using handcrafted features [135], [138], dynamic time warping [119], temporal information [17], [146] as well as temporal pyramids [108], [149]. With the resurgence of deep learning, all these methods have been quickly overtaken by 2D/3D Convolutional Neural Networks (CNNs) [31], [93], [100] that capture global skeleton posture together with local joint motion [38], [79], by Recurrent Neural Networks (RNNs) which capture motion dynamics [8], [14], [54], [65], [82], [83], [85], [86], [88], [92], [101], [113], [121], [127], [143], [144], [149], and manifold learning [45], [47], [53], [80], [98] as well as attention-based networks [10], [38], [116], [131]. With the recent emergence of GCNs, the latter have been increasingly used in skeleton-based recognition [45], [46], [70], [72], [76], [98], [115], [129], [136]. These models explicitly capture, with a better interpretability, spatial and temporal attention among skeleton joints [74]. However, on tasks involving large input graphs (such skeleton-based recognition), GCNs become computationally inefficient and require lightweight design techniques.

3 PROPOSED METHOD

GCNs correspond to convolutional blocks with two layers; the first one aggregates signals (through adjacency matrices) while the second layer achieves convolution by multiplying the resulting aggregates with filters. Learning multiple adjacency (also referred to as attention) matrices allows us to capture different contexts and graph topologies when achieving aggregation and convolution. Stacking aggregation and convolutional layers, with multiple attention matrices, makes GCNs accurate but heavy. We propose, in what follows, a method that makes our networks lightweight and still effective.

We formally subsume a given GCN as a multi-layered neural network g_θ whose weights are defined as $\theta = \{\mathbf{W}^1, \dots, \mathbf{W}^L\}$, with L being its depth, $\mathbf{W}^\ell \in \mathbb{R}^{d_{\ell-1} \times d_\ell}$ its ℓ^{th} layer weight tensor, and d_ℓ the dimension of ℓ . The output of a layer ℓ is $\phi^\ell = f_\ell(\mathbf{W}^{\ell \top} \phi^{\ell-1})$, $\ell \in \{2, \dots, L\}$, with f_ℓ being an activation function.

We consider a *parametrization*, related to magnitude pruning, that allows defining both the topology of the pruned networks and their weights. This parametrization corresponds to the Hadamard product of a weight tensor and a function applied entry-wise to the same tensor as

$$\mathbf{W}^\ell = \hat{\mathbf{W}}^\ell \odot \psi(\hat{\mathbf{W}}^\ell), \quad (1)$$

here $\hat{\mathbf{W}}^\ell$ is a latent tensor and $\psi(\hat{\mathbf{W}}^\ell)$ is a continuous relaxation of the binary masks which enforces the prior that smallest weights should be removed from the network. A possible choice, used in practice, is $\psi_{a,\sigma}(\hat{\mathbf{w}}) = (1 + \sigma \exp(a^2 - \hat{\mathbf{w}}^2))^{-1}$ being σ a scaling factor and “ a ” threshold. As illustrated in Fig. 1, σ controls the smoothness of $\psi_{a,\sigma}$ around the support $\Omega \subseteq \mathbb{R}$ of the latent

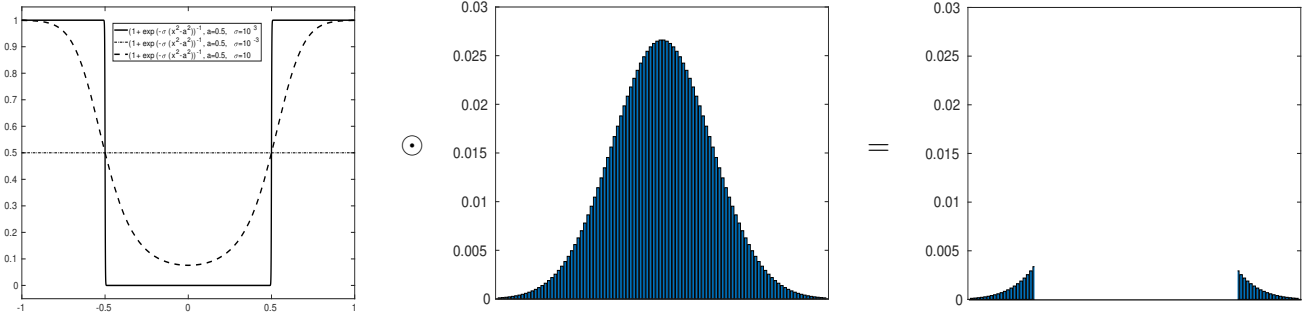


Fig. 1. This figure shows a Band-stop function $\psi_{a,\sigma}$ applied to a given (gaussian) weight distribution. Depending on a , only weights with large magnitudes are kept (Better to zoom the file).

weights. This makes it possible to implement an annealed thresholding function that removes connections in a smooth and differentiable manner as training of the latent parameters evolves. In other words, the asymptotic behavior of $\psi_{a,\sigma}$ — that allows defining the topology of the pruned networks — is obtained as training reaches the final epochs.

3.1 SRMP: Single-Rate Magnitude Pruning

The parameterization described above — despite being effective (as shown later in experiments) — does not allow to implement any a priori fixed pruning rate as the dynamic of the weights $\{\hat{\mathbf{W}}^\ell\}_\ell$ is not known beforehand. Hence, pruning rates could only be observed a posteriori or implemented after training using, for instance, a two stage process (namely magnitude pruning + fine-tuning). In order to implement any targeted pruning rate in one training step, the distribution of latent weights is constrained to fit an arbitrary fixed probability distribution, so one may set a in $\psi_{a,\sigma}$ and hence implement the a priori fixed pruning rate. Let $\hat{W} \in \Omega$ be a random variable standing for the latent weights in g_θ ; \hat{W} is assumed taken from any arbitrary distribution P (uniform, gaussian, laplace, etc). Setting appropriately P (not only) makes it possible to implement any targeted pruning rate, but also acts as a regularizer that controls the dynamic of the learned weights and thereby the generalization of g_θ as shown subsequently and also observed in experiments.

Let Q be the observed distribution of $\{\hat{\mathbf{W}}^\ell\}_\ell$, and P the targeted (fixed) one, our objective is to reduce the difference between P and Q using a Kullback-Leibler Divergence (KLD) criterion $D_{KL}(P||Q)$. Notice that the analytic form of $D_{KL}(P||Q)$ is known on the widely used PDFs (probability density functions), whilst for any arbitrary PDF, the exact form is not always known. Hence, we consider instead an empirical (discrete) variant of this criterion and also P, Q ; here P is again the targeted distribution (such as gaussian, laplace and uniform) while the observed (and also differentiable) one Q is based on a relaxed histogram estimation. Let $\{q_1, \dots, q_K\}$ be a K -bin quantization of Ω ($K = 100$ in practice), the k -th entry of Q is given by

$$Q(\hat{W} = q_k) \propto \sum_{\ell=1}^{L-1} \sum_{i=1}^{n_\ell} \sum_{j=1}^{n_{\ell+1}} \exp \left\{ -(\hat{\mathbf{W}}_{i,j}^\ell - q_k)^2 / \beta_k^2 \right\}, \quad (2)$$

here β_k is a scaling coefficient whose value controls the smoothness of the exponential; high β_k results into flat (oversmoothed) histograms while a sufficiently (but not very) small β_k allows obtaining surrogate histograms similar to the actual distribution of Q . In practice, β_k is fixed to $(q_{k+1} - q_k)/2$; with this β_k , the partition function of Q — i.e., $\sum_{k=1}^K Q(\hat{W} = q_k)$ — reaches almost

one in practice, so one may replace \propto (in Eq. 2) with equality.

Considering $F_{\hat{W}}(a) = P(\hat{W} \leq a)$ as the cumulative distribution function (CDF) of $P(\hat{W})$. For any fixed pruning rate r , one may set the threshold a of $\psi_{a,\sigma}$ as

$$a(r) = F_{\hat{W}}^{-1}(r), \quad (3)$$

which corresponds to the quantile that defines the pruning threshold on the targeted distribution P (and also on the observed distribution Q thanks to KLD). This guarantees that only a fraction r of the total weights are removed when applying the band-stop in Eq. 1. It's worth noticing that the quantile at any given r , can either be analytically derived on the widely used PDFs or empirically evaluated on discrete random variables.

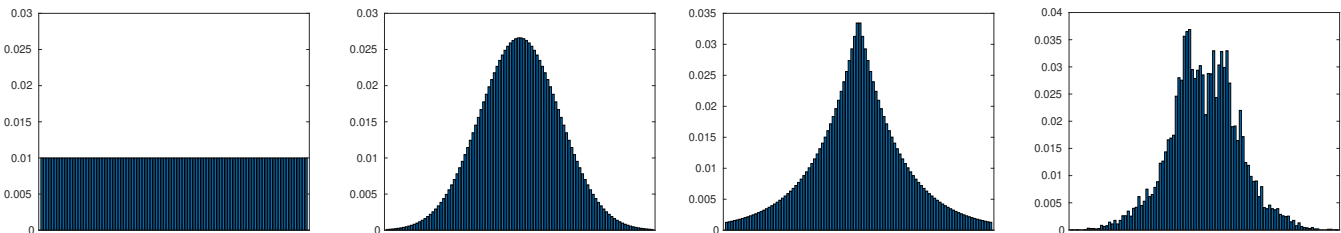


Fig. 2. From left to right: the 3 figures correspond to targeted (uniform, gaussian and laplace) distributions, and the 4th figure shows the actual weight distribution of the unpruned GCN which resembles to gaussian/laplacian.

Following the aforementioned budget implementation, pruning is achieved using an objective function that mixes a cross-entropy term \mathcal{L}_e , and the KLD criterion D_{KL} resulting into

$$\min_{\{\hat{\mathbf{W}}^\ell\}_\ell} \mathcal{L}_e(\{\hat{\mathbf{W}}^\ell \odot \psi_{a,\sigma}(\hat{\mathbf{W}}^\ell)\}_\ell) + \lambda D_{KL}(P||Q), \quad (4)$$

again KLD controls weight distribution and it guarantees the targeted pruning budget depending on a in $\psi_{a,\sigma}$ as shown in Eq. 3. In the above objective function, λ is overestimated (to 10 in practice) in order to make Eq. 4 focusing on the implementation of the budget. As training reaches its final epochs, D_{KL} reaches its minimum and the gradient of the global objective function becomes dominated by the gradient of \mathcal{L}_e , and this allows improving further classification performances.

3.2 MRMP: Multi-Rate Magnitude Pruning

The aforementioned formulation is already effective (see later experiments), however, it requires rerunning a complete optimization, for any update of the pruning rate which is time and memory demanding. In what follows, we introduce a framework that allows training GCN instances with *shared latent weights* which achieve optimal performances at multiple pruning rates without retraining.

The guiding principle of our method relies on sharing the latent weights $\{\hat{\mathbf{W}}^\ell\}_\ell$ through multiple GCN instances defined by the hyperparameters $\{a(r)\}_r$ in $\psi_{a,\sigma}$. This makes it possible to reduce not only training time (as a unique training session is necessary for all the pruning rates) but also the memory footprint as the number of latent weights remains unchanged. Furthermore, training multiple GCN instances on top of shared latent parameters makes each instance as a proxy task to the other GCN learning tasks, and this turns out to improve generalization as shown in experiments. Last but not least, this also allows obtaining optimal pruned networks

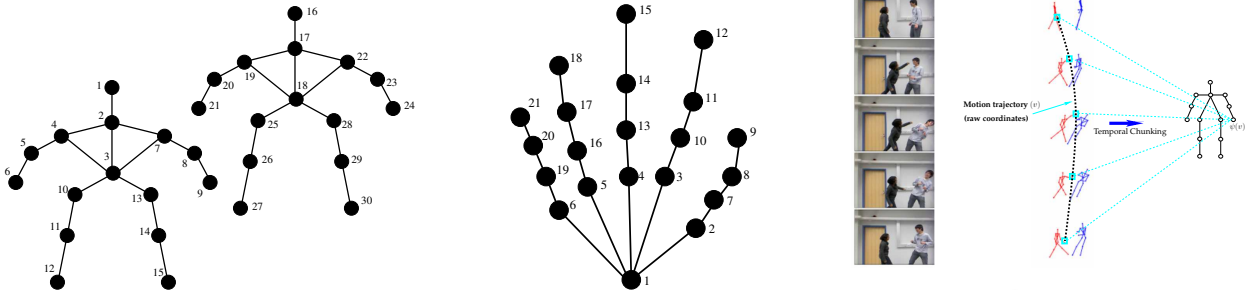


Fig. 3. This figure shows original skeletons (left) on the SBU and (middle) the FPHA datasets. (Right) this figure shows the whole keypoint tracking and description process.

(at unseen pruning rates) instantaneously without retraining. In order to achieve these goals, we propose an updated loss as

$$\min_{\{\hat{\mathbf{W}}^\ell\}_\ell} \sum_r \mathcal{L}_e(\{\hat{\mathbf{W}}^\ell \odot \psi_{a(r),\sigma}(\hat{\mathbf{W}}^\ell)\}_\ell) + \lambda D_{KL}(P||Q), \quad (5)$$

here the right-hand side term remains unchanged and it again seeks to constrain the latent weights to fit a targeted distribution. In contrast, the left-hand side (cross entropy) term, is evaluated through multiple pruning rates using the shared latent weights; hence only $\psi_{a(r),\sigma}$ intervenes in order to prune connections according to the targeted rates. Once the optimization achieved, GCN instances may be obtained at any fixed pruning rates (including unseen ones) by multiplying each weight tensor with the binary mask tensor as $\{\hat{\mathbf{W}}^\ell \odot \psi_{a,\sigma}(\hat{\mathbf{W}}^\ell)\}_\ell$ here a is again obtained using Eq. 3 and thanks to the KLD criterion in Eq.5. It's worth noticing that the computational complexity of the above formulation is highly efficient (compared to running multiple independent instances of pruning); indeed, the gradient of the KLD term is exactly the same while all the gradients of the left-hand side terms (w.r.t. the GCN output) have similar analytic forms and their evaluation for different r (either during forward and backward steps of backpropagation) could be batched and efficiently vectorized. In practice, we observe a slight overhead of MRMP against SRMP (Single Rate Magnitude Pruning), in forward and backward steps, even when one hundred pruning rates (r) are jointly considered for MRMP.

4 EXPERIMENTS

In this section, we evaluate the performance of our baseline and pruned GCNs on the task of skeleton-based recognition using two challenging skeleton datasets; SBU Interaction [140] and First-Person Hand Action (FPHA) [19]. The goal is to study the performance of our lightweight GCN design and its comparison against staple pruning techniques as well as the related work.

Dataset description. SBU is an interaction dataset acquired (under relatively well controlled conditions) using the Microsoft Kinect sensor; it includes in total 282 moving skeleton sequences (performed by two interacting individuals) belonging to 8 categories: “approaching”, “departing”, “pushing”, “kicking”, “punching”, “exchanging objects”, “hugging”, and “hand shaking”. Each pair of interacting individuals corresponds to two 15 joint skeletons and each joint is encoded with a sequence of its 3D coordinates across video frames. In this dataset, we consider the same evaluation protocol as the one suggested in the original dataset release [140] (i.e., train-test split).

The FPHA dataset includes 1175 skeletons belonging to 45 action categories which are performed

Method	Accuracy (%)
Raw Position [140]	49.7
Joint feature [49]	86.9
CHARM [77]	86.9
H-RNN [14]	80.4
ST-LSTM [82]	88.6
Co-occurrence-LSTM [149]	90.4
STA-LSTM [116]	91.5
ST-LSTM + Trust Gate [82]	93.3
VA-LSTM [143]	97.6
GCA-LSTM [83]	94.9
Riemannian manifold. traj [53]	93.7
DeepGRU [92]	95.7
RHCN + ACSC + STUFE [76]	98.7
Our baseline GCN	98.4

TABLE 1
Comparison of our baseline GCN against related work on the SBU database.

by 6 different individuals in 3 scenarios. In contrast to SBU, action categories are highly variable with inter and intra subject variability including style, speed, scale and viewpoint. Each skeleton includes 21 hand joints and each joint is again encoded with a sequence of its 3D coordinates across video frames. We evaluate the performance of our method using the 1:1 setting proposed in [19] with 600 action sequences for training and 575 for testing. In all these experiments, we report the average accuracy over all the classes of actions.

Skeleton normalization. Let $S^t = \{p_1^t, \dots, p_n^t\}$ denote the 3D skeleton coordinates at frame t . Without a loss of generality, we consider a particular order so that p_1^t , p_2^t and p_3^t correspond to three reference joints (e.g., neck, left shoulder and right shoulder); as shown in Fig. 3, this corresponds to joints 2, 4 and 7 for SBU and 1, 3 and 5 for FPHA. As the relative distance between these 3 joints is stable w.r.t. any motion, these 3 joints are used in order to estimate the rigid motion (similarity transformation) for skeleton normalization; see also [95]. Each graph sequence is processed in order to normalize its 3D coordinates using a similarity transformation; the translation parameters $\mathbf{t} = (t_x, t_y, t_z)$ of this transformation correspond to the shift that makes the reference point $(p_2^0 + p_3^0)/2$ coincide with the origin while the rotation parameters $(\theta_x, \theta_y, \theta_z)$ are chosen in order to make the plane formed by p_1^0 , p_2^0 and p_3^0 coplanar with the x-y plane and the vector $p_2^0 - p_3^0$ colinear with the x-axis. Finally, the scaling γ of this similarity is chosen to make the $\|p_2^0 - p_3^0\|_2$ constant through all the action instances. Hence, each normalized joint is transformed as $\hat{p}_i^t = \gamma(p_i^t - \mathbf{t})R_x(\theta_x)R_y(\theta_y)R_z(\theta_z)$ with R_x , R_y , R_z being rotation matrices along the x , y and z axes respectively.

Input graphs. Considering a sequence of normalized skeletons $\{S^t\}_t$, each joint sequence $\{\hat{p}_j^t\}_t$ in these skeletons defines a labeled trajectory through successive frames (see Fig. 3-right). Given a finite collection of trajectories, we consider the input graph $\mathcal{G} = (\mathcal{V}, \mathcal{E})$ where each node $v_j \in \mathcal{V}$ corresponds to the labeled trajectory $\{\hat{p}_j^t\}_t$ and an edge $(v_j, v_i) \in \mathcal{E}$ exists between two nodes iff the underlying trajectories are spatially neighbors. Each trajectory (i.e., node in \mathcal{G}) is processed using *temporal chunking*: first, the total duration of a sequence (video) is split into M equally-sized temporal chunks ($M = 4$ in practice), then the normalized joint coordinates $\{\hat{p}_j^t\}_t$ of the trajectory v_j are assigned to the M chunks (depending on their time stamps) prior to concatenate

the averages of these chunks; this produces the description of v_j (again denoted as $\phi(v_j) \in \mathbb{R}^s$ with $s = 3 \times M$) and $\{\phi(v_j)\}_j$ constitutes the raw signal of nodes in a given sequence. Note that two trajectories v_j and v_i , with similar joint coordinates but arranged differently in time, will be considered as very different when using temporal chunking. Note that temporal chunking produces discriminant raw descriptions that preserve the temporal structure of trajectories while being *frame-rate* and *duration* agnostic.

Method	Color	Depth	Pose	Accuracy (%)
2-stream-color [31]	✓	✗	✗	61.56
2-stream-flow [31]	✓	✗	✗	69.91
2-stream-all [31]	✓	✗	✗	75.30
HOG2-dep [103]	✗	✓	✗	59.83
HOG2-dep+pose [103]	✗	✓	✓	66.78
HON4D [105]	✗	✓	✗	70.61
Novel View [109]	✗	✓	✗	69.21
1-layer LSTM [149]	✗	✗	✓	78.73
2-layer LSTM [149]	✗	✗	✓	80.14
Moving Pose [141]	✗	✗	✓	56.34
Lie Group [119]	✗	✗	✓	82.69
HBRNN [14]	✗	✗	✓	77.40
Gram Matrix [146]	✗	✗	✓	85.39
TF [17]	✗	✗	✓	80.69
JOULE-color [42]	✓	✗	✗	66.78
JOULE-depth [42]	✗	✓	✗	60.17
JOULE-pose [42]	✗	✗	✓	74.60
JOULE-all [42]	✓	✓	✓	78.78
Huang et al. [45]	✗	✗	✓	84.35
Huang et al. [47]	✗	✗	✓	77.57
HAN [80]	✗	✗	✓	85.74
Our baseline GCN	✗	✗	✓	86.43

TABLE 2

Comparison of our baseline GCN against related work on the FPHA database.

Implementation details & baseline GCNs. We trained the GCN networks end-to-end using the Adam optimizer [57] for 2,700 epochs with a batch size equal to 200 for SBU and 600 for FPHA, a momentum of 0.9 and a global learning rate (denoted as $\nu(t)$) inversely proportional to the speed of change of the loss used to train our networks; when this speed increases (resp. decreases), $\nu(t)$ decreases as $\nu(t) \leftarrow \nu(t-1) \times 0.99$ (resp. increases as $\nu(t) \leftarrow \nu(t-1)/0.99$). All these experiments are run on a GeForce GTX 1070 GPU device (with 8 GB memory) and neither dropout nor data augmentation are used. The architecture of our baseline GCN includes an attention layer of 1 head on SBU (resp. 16 heads on FPHA) applied to skeleton graphs whose nodes are encoded with 8-channels (resp. 32 for FPHA), followed by a convolutional layer of 32 filters for SBU (resp. 128 filters for FPHA), and a dense fully connected layer and a softmax layer. The initial network for SBU is not very heavy, its number of parameters does not exceed 15,320, and this makes its pruning challenging as many connections will be isolated (not contributing in the evaluation of the network output). In contrast, the initial network for FPHA is relatively heavy (for a GCN) and its number of parameters reaches 2 millions. As shown in tables. 1 and 2, both GCNs are accurate compared to the related work on the SBU/FPHA benchmarks. Considering these GCN baselines,

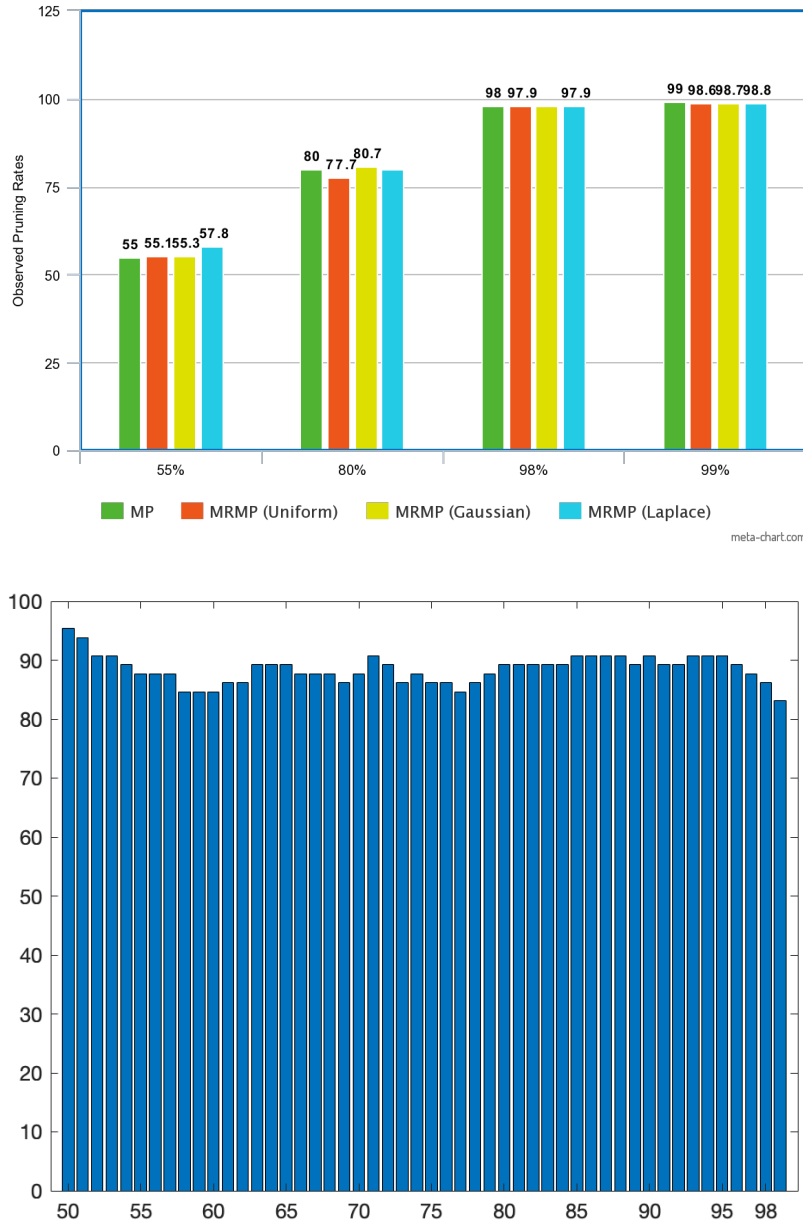


Fig. 4. Performances on the SBU dataset: (Top) Fixed and observed pruning rates when different PDFs are used in the KLD regularizer. (Bottom) Performances for different (seen and unseen) pruning rates of MRMP; again seen pruning rates (during training) correspond to 50, 55, 60, 65, 70, 75, 80, 85, 90, 95 and 98% while unseen ones correspond to all the remaining pruning rates in $[50, 100]$. Better to zoom the file.

our goal is to make them highly lightweight while making their accuracy as high as possible.

Performances, Comparison & Ablation. Tables 3-4 and Fig. 4 show a comparison and an ablation study of our method both on SBU and FPHA datasets. First, from the results in Fig.4-top, we see the alignment between the targeted pruning rates and the observed ones when using the formulation in Eq. 4 for different PDFs; the quantile functions of the gaussian and laplace PDFs allow implementing *fine-steps* of the targeted pruning rates r particularly when r is large. In contrast, the quantile functions of the gaussian and laplace PDFs are coarse around mid r values (55%). Second, according to tables 3-4, when training is achieved with only the band-stop

Pruning rates	Accuracy (%)	Observation
0%	98.40	Baseline GCN
70%	93.84	Band-stop Weight Param.
	89.23	MP
	83.07	SRMP: MP+KLD (Uniform)
	93.84	MRMP: MP+KLD (Uniform)+MR
55%	81.53	SRMP: MP+KLD (Gaussian)
	90.76	MRMP: MP+KLD (Gaussian)+MR
	80.00	SRMP: MP+KLD (Laplace)
	89.23	MRMP: MP+KLD (Laplace)+MR
	87.69	MP
	84.61	SRMP: MP+KLD (Uniform)
	89.23	MRMP: MP+KLD (Uniform)+MR
80%	78.46	SRMP: MP+KLD (Gaussian)
	89.23	MRMP: MP+KLD (Gaussian)+MR
	80.00	SRMP: MP+KLD (Laplace)
	90.76	MRMP: MP+KLD (Laplace)+MR
	69.23	MP
	78.46	SRMP: MP+KLD (Uniform)
	86.15	MRMP: MP+KLD (Uniform)+MR
98%	47.69	SRMP: MP+KLD (Gaussian)
	86.15	MRMP: MP+KLD (Gaussian)+MR
	60.00	SRMP: MP+KLD (Laplace)
	80.00	MRMP: MP+KLD (Laplace)+MR
Comparative (regularization-based) pruning		
	55.38	MP+ ℓ_0 -reg.
98%	73.84	MP+ ℓ_1 -reg.
	61.53	MP+Entropy-reg.
	75.38	MP+Cost-aware-reg.

TABLE 3

Detailed performances and ablation study on SBU, for different pruning rates, PDFs used for KLD and also MR; MR stands for Multi-Rate pruning.

weight parametrization (i.e., $\lambda = 0$ in Eq. 4), performances are close to the initial heavy GCNs (particularly on FPHA), with less parameters¹ as this produces a regularization effect similar to [120]. Third, we observe a positive impact when the KLD term (in Eq. 4) is used both with single and multi-rate magnitude pruning (resp. SRMP and MRMP) with an extra-advantage of MRMP against SRMP; again MP+KLD in tables 3-4 corresponds to SRMP and MP+KLD+MR refers to MRMP. Extra comparison of KLD against other regularizers shows the substantial gain of our method. Indeed, KLD is compared against different alternatives plugged in Eq. 4 instead of KLD, namely ℓ_0 [90], ℓ_1 [61], entropy [132] and ℓ_2 -based cost [67]. From the observed results, the impact of KLD is substantial for different PDFs and for equivalent pruning rate (namely 98%). Note that when alternative regularizers are used, multiple settings (trials) of the underlying hyperparameter λ (in Eq. 4) are considered prior to reach the targeted pruning rate, and this makes the whole training and pruning process overwhelming. While cost-aware regularization makes training more tractable, its downside resides in the observed collapse of trained masks; this is a well known effect that affects performances at high pruning rates. Finally, Fig.4-bottom

1. Pruning rate does not exceed 70% and no control on this rate is achievable.

Pruning rates	Accuracy (%)	Observation
0%	86.43	Baseline GCN
50%	85.56	Band-stop Weight Param.
	87.82	MP
	87.82	SRMP: MP+KLD (Uniform)
	88.92	MRMP: MP+KLD (Uniform)+MR
55%	88.52	SRMP: MP+KLD (Gaussian)
	89.58	MRMP: MP+KLD (Gaussian)+MR
	87.65	SRMP: MP+KLD (Laplace)
	88.48	MRMP: MP+KLD (Laplace)+MR
	86.78	MP
	85.91	SRMP: MP+KLD (Uniform)
	86.43	MRMP: MP+KLD (Uniform)+MR
80%	87.47	SRMP: MP+KLD (Gaussian)
	88.93	MRMP: MP+KLD (Gaussian)+MR
	86.95	SRMP: MP+KLD (Laplace)
	87.89	MRMP: MP+KLD (Laplace)+MR
	60.34	MP
	70.26	SRMP: MP+KLD (Uniform)
	71.18	MRMP: MP+KLD (Uniform)+MR
98%	70.60	SRMP: MP+KLD (Gaussian)
	74.73	MRMP: MP+KLD (Gaussian)+MR
	70.80	SRMP: MP+KLD (Laplace)
	72.97	MRMP: MP+KLD (Laplace)+MR
Comparative (regularization-based) pruning		
	64.69	MP+ ℓ_0 -reg.
98%	70.78	MP+ ℓ_1 -reg.
	67.47	MP+Entropy-reg.
	69.91	MP+Cost-aware-reg.

TABLE 4
Same caption as tab 3 but for FPHA dataset.

shows the generalization performance of MRMP from seen to unseen pruning rates. In these results, only a few pruning rates are used for MRMP (namely 50, 55, 60, 65, 70, 75, 80, 85, 90, 95 and 98%) and all the remaining rates in $[50, 100[$ are used for instantaneous pruning without retraining. We observe stable and high performances *from seen to unseen* pruning rates and this shows that MRMP is able to extrapolate highly accurate GCNs (even) on unseen pruning rates.

5 CONCLUSION

We introduce in this paper a novel lightweight GCN design based on multi-rate magnitude pruning. Our method allows training multiple network instances simultaneously, on top of shared latent weights, at different pruning rates and extrapolating GCNs at unseen rates without retraining their weights. Experiments conducted on the challenging task of skeleton-based recognition, using two different standard datasets, show a significant gain of our method against the related work. As a perspective, we are currently investigating the extension of the current approach to other deep neural architectures and applications.

REFERENCES

- [1] Sungsoo Ahn, Shell Xu Hu, Andreas Damianou, Neil D Lawrence, and Zhenwen Dai. Variational information distillation for knowledge transfer. In *Proceedings of the IEEE/CVF Conference on Computer Vision and Pattern Recognition*, pages 9163–9171, 2019.
- [2] H. Sahbi and N. Boujemaa. “From coarse to fine skin and face detection.” *Proceedings of the eighth ACM international conference on Multimedia*. 2000.
- [3] Joan Bruna, Wojciech Zaremba, Arthur Szlam, and Yann LeCun. Spectral networks and locally connected networks on graphs. *arXiv preprint arXiv:1312.6203*, 2013.
- [4] Han Cai, Chuang Gan, Tianzhe Wang, Zhekai Zhang, and Song Han. Once-for-all: Train one network and specialize it for efficient deployment. *arXiv preprint arXiv:1908.09791*, 2019.
- [5] H. Sahbi and F. Fleuret. Scale-invariance of support vector machines based on the triangular kernel. Diss. INRIA, 2002.
- [6] Zhe Cao, Tomas Simon, Shih-En Wei, and Yaser Sheikh. Realtime multi-person 2d pose estimation using part affinity fields. In *Proceedings of the IEEE conference on computer vision and pattern recognition*, pages 7291–7299, 2017.
- [7] Miguel A Carreira-Perpinán and Yerlan Idelbayev. “learning-compression” algorithms for neural net pruning. In *Proceedings of the IEEE Conference on Computer Vision and Pattern Recognition*, pages 8532–8541, 2018.
- [8] Xinghao Chen, Hengkai Guo, Guijin Wang, and Li Zhang. Motion feature augmented recurrent neural network for skeleton-based dynamic hand gesture recognition. In *2017 IEEE International Conference on Image Processing (ICIP)*, pages 2881–2885. IEEE, 2017.
- [9] L. Wang and H. Sahbi. “Nonlinear cross-view sample enrichment for action recognition.” *European Conference on Computer Vision*. Springer, Cham, 2014.
- [10] Yuxiao Chen, Long Zhao, Xi Peng, Jianbo Yuan, and Dimitris N Metaxas. Construct dynamic graphs for hand gesture recognition via spatial-temporal attention. *arXiv preprint arXiv:1907.08871*, 2019.
- [11] Fan RK Chung. *Spectral graph theory*, volume 92. American Mathematical Soc., 1997.
- [12] M. Ferencat and H. Sahbi. “Multi-view object matching and tracking using canonical correlation analysis.” 2009 16th IEEE International Conference on Image Processing (ICIP). IEEE, 2009.
- [13] Michaël Defferrard, Xavier Bresson, and Pierre Vandergheynst. Convolutional neural networks on graphs with fast localized spectral filtering. *Advances in neural information processing systems*, 29, 2016.
- [14] Yong Du, Wei Wang, and Liang Wang. Hierarchical recurrent neural network for skeleton based action recognition. In *Proceedings of the IEEE conference on computer vision and pattern recognition*, pages 1110–1118, 2015.
- [15] H. Sahbi, L. Ballan, G. Serra, A. Del-Bimbo. Context-dependent logo matching and recognition. *IEEE Transactions on Image Processing* 22 (3), 1018-1031.
- [16] Christoph Feichtenhofer, Axel Pinz, and Andrew Zisserman. Convolutional two-stream network fusion for video action recognition. In *Proceedings of the IEEE conference on computer vision and pattern recognition*, pages 1933–1941, 2016.
- [17] Guillermo Garcia-Hernando and Tae-Kyun Kim. Transition forests: Learning discriminative temporal transitions for action recognition and detection. In *Proceedings of the IEEE Conference on Computer Vision and Pattern Recognition*, pages 432–440, 2017.
- [18] H. Sahbi. “Misalignment resilient cca for interactive satellite image change detection.” 2016 23rd International Conference on Pattern Recognition (ICPR). IEEE, 2016.
- [19] Guillermo Garcia-Hernando, Shanxin Yuan, Seungryul Baek, and Tae-Kyun Kim. First-person hand action benchmark with rgb-d videos and 3d hand pose annotations. In *Proceedings of the IEEE conference on computer vision and pattern recognition*, pages 409–419, 2018.
- [20] Ariel Gordon, Elad Eban, Ofir Nachum, Bo Chen, Hao Wu, Tien-Ju Yang, and Edward Choi. Morphnet: Fast & simple resource-constrained structure learning of deep networks. In *Proceedings of the IEEE conference on computer vision and pattern recognition*, pages 1586–1595, 2018.
- [21] Marco Gori, Gabriele Monfardini, and Franco Scarselli. A new model for learning in graph domains. In *Proceedings. 2005 IEEE International Joint Conference on Neural Networks, 2005.*, volume 2, pages 729–734. IEEE, 2005.
- [22] T. Napoléon and H. Sahbi. “From 2D silhouettes to 3D object retrieval: contributions and benchmarking.” *EURASIP Journal on Image and Video Processing* 2010 (2010): 1-17.
- [23] Will Hamilton, Zhitao Ying, and Jure Leskovec. Inductive representation learning on large graphs. *Advances in neural information processing systems*, 30, 2017.
- [24] Song Han, Huizi Mao, and William J Dally. Deep compression: Compressing deep neural networks with pruning, trained quantization and Huffman coding. *arXiv preprint arXiv:1510.00149*, 2015.
- [25] X. Li and H. Sahbi. “Superpixel-based object class segmentation using conditional random fields.” 2011 IEEE International Conference on Acoustics, Speech and Signal Processing (ICASSP). IEEE, 2011.
- [26] Song Han, Jeff Pool, John Tran, and William Dally. Learning both weights and connections for efficient neural network. *Advances in neural information processing systems*, 28, 2015.
- [27] Babak Hassibi and David Stork. Second order derivatives for network pruning: Optimal brain surgeon. *Advances in neural information processing systems*, 5, 1992.

- [28] M. Jiu and H. Sahbi. "Semi supervised deep kernel design for image annotation." 2015 IEEE International Conference on Acoustics, Speech and Signal Processing (ICASSP). IEEE, 2015.
- [29] Kaiming He, Georgia Gkioxari, Piotr Dollár, and Ross Girshick. Mask r-cnn. In *Proceedings of the IEEE international conference on computer vision*, pages 2961–2969, 2017.
- [30] Kaiming He, Xiangyu Zhang, Shaoqing Ren, and Jian Sun. Deep residual learning for image recognition. In *Proceedings of the IEEE conference on computer vision and pattern recognition*, pages 770–778, 2016.
- [31] M. Jiu and H. Sahbi. "Deep kernel map networks for image annotation." 2016 IEEE International Conference on Acoustics, Speech and Signal Processing (ICASSP). IEEE, 2016.
- [32] Yang He, Guoliang Kang, Xuanyi Dong, Yanwei Fu, and Yi Yang. Soft filter pruning for accelerating deep convolutional neural networks. *arXiv preprint arXiv:1808.06866*, 2018.
- [33] Yihui He, Ji Lin, Zhijian Liu, Hanrui Wang, Li-Jia Li, and Song Han. Amc: Automl for model compression and acceleration on mobile devices. In *Proceedings of the European conference on computer vision (ECCV)*, pages 784–800, 2018.
- [34] H. Sahbi, Jean-Yves Audibert, and Renaud Keriven. "Graph-cut transducers for relevance feedback in content based image retrieval." 2007 IEEE 11th International Conference on Computer Vision. IEEE, 2007.
- [35] Mikael Henaff, Joan Bruna, and Yann LeCun. Deep convolutional networks on graph-structured data. *arXiv preprint arXiv:1506.05163*, 2015.
- [36] Geoffrey Hinton, Oriol Vinyals, and Jeff Dean. Distilling the knowledge in a neural network. *arXiv preprint arXiv:1503.02531*, 2015.
- [37] H. Sahbi, S. Deschamps, A. Stoian. Frugal Learning for Interactive Satellite Image Change Detection. IEEE IGARSS, 2021.
- [38] Jingxuan Hou, Guijin Wang, Xinghao Chen, Jing-Hao Xue, Rui Zhu, and Huazhong Yang. Spatial-temporal attention res-tcn for skeleton-based dynamic hand gesture recognition. In *Proceedings of the European conference on computer vision (ECCV) workshops*, pages 0–0, 2018.
- [39] Andrew Howard, Mark Sandler, Grace Chu, Liang-Chieh Chen, Bo Chen, Mingxing Tan, Weijun Wang, Yukun Zhu, Ruoming Pang, Vijay Vasudevan, et al. Searching for mobilenet3. In *Proceedings of the IEEE/CVF international conference on computer vision*, pages 1314–1324, 2019.
- [40] Andrew G Howard, Menglong Zhu, Bo Chen, Dmitry Kalenichenko, Weijun Wang, Tobias Weyand, Marco Andreetto, and Hartwig Adam. Mobilenets: Efficient convolutional neural networks for mobile vision applications. *arXiv preprint arXiv:1704.04861*, 2017.
- [41] S. Thiemert, H. Sahbi, and M. Steinebach. "Applying interest operators in semi-fragile video watermarking." Security, Steganography, and Watermarking of Multimedia Contents VII. Vol. 5681. SPIE, 2005.
- [42] Jian-Fang Hu, Wei-Shi Zheng, Jianhuang Lai, and Jianguo Zhang. Jointly learning heterogeneous features for rgb-d activity recognition. In *Proceedings of the IEEE conference on computer vision and pattern recognition*, pages 5344–5352, 2015.
- [43] Gao Huang, Shichen Liu, Laurens Van der Maaten, and Kilian Q Weinberger. Condensenet: An efficient densenet using learned group convolutions. In *Proceedings of the IEEE conference on computer vision and pattern recognition*, pages 2752–2761, 2018.
- [44] H. Sahbi. "Imageclef annotation with explicit context-aware kernel maps." International Journal of Multimedia Information Retrieval 4.2 (2015): 113-128.
- [45] Zhiwu Huang and Luc Van Gool. A riemannian network for spd matrix learning. In *Proceedings of the AAAI conference on artificial intelligence*, volume 31, 2017.
- [46] Zhiwu Huang, Chengde Wan, Thomas Probst, and Luc Van Gool. Deep learning on lie groups for skeleton-based action recognition. In *Proceedings of the IEEE conference on computer vision and pattern recognition*, pages 6099–6108, 2017.
- [47] Zhiwu Huang, Jiqing Wu, and Luc Van Gool. Building deep networks on grassmann manifolds. In *Proceedings of the AAAI Conference on Artificial Intelligence*, volume 32, 2018.
- [48] H. Sahbi. "CNRS-TELECOM ParisTech at ImageCLEF 2013 Scalable Concept Image Annotation Task: Winning Annotations with Context Dependent SVMs." CLEF (Working Notes). 2013.
- [49] Yanli Ji, Guo Ye, and Hong Cheng. Interactive body part contrast mining for human interaction recognition. In *2014 IEEE international conference on multimedia and expo workshops (ICMEW)*, pages 1–6. IEEE, 2014.
- [50] WEN Jian, Yujie Zhou, and Hongming Liu. Densely connected convolutional network optimized by genetic algorithm for fingerprint liveness detection. *IEEE Access*, 9:2229–2243, 2020.
- [51] H. Sahbi. A particular Gaussian mixture model for clustering and its application to image retrieval. *Soft Computing* 12 (7), 667-676
- [52] Mingyuan Jiu and Hichem Sahbi. Deep representation design from deep kernel networks. *Pattern Recognition*, 88:447–457, 2019.
- [53] Anis Kacem, Mohamed Daoudi, Boulbaba Ben Amor, Stefano Berretti, and Juan Carlos Alvarez-Paiva. A novel geometric framework on gram matrix trajectories for human behavior understanding. *IEEE transactions on pattern analysis and machine intelligence*, 42(1):1–14, 2018.
- [54] QiuHong Ke, Mohammed Bennamoun, Senjian An, Ferdous Sohel, and Farid Boussaid. A new representation of skeleton sequences for 3d action recognition. In *Proceedings of the IEEE conference on computer vision and pattern recognition*, pages 3288–3297, 2017.

- [55] A. Mazari and H. Sahbi. "MLGCN: Multi-Laplacian graph convolutional networks for human action recognition." The British Machine Vision Conference (BMVC). 2019.
- [56] Leonid Keselman, John Iselin Woodfill, Anders Grunnet-Jepsen, and Achintya Bhowmik. Intel realsense stereoscopic depth cameras. In *Proceedings of the IEEE conference on computer vision and pattern recognition workshops*, pages 1–10, 2017.
- [57] Diederik P Kingma and Jimmy Ba. Adam: A method for stochastic optimization. *arXiv preprint arXiv:1412.6980*, 2014.
- [58] Thomas N Kipf and Max Welling. Semi-supervised classification with graph convolutional networks. *arXiv preprint arXiv:1609.02907*, 2016.
- [59] M. Ferecatu and H. Sahbi. "TELECOM ParisTech at ImageClefphoto 2008: Bi-Modal Text and Image Retrieval with Diversity Enhancement." CLEF (Working Notes). 2008.
- [60] Boris Knyazev, Graham W Taylor, and Mohamed Amer. Understanding attention and generalization in graph neural networks. *Advances in neural information processing systems*, 32, 2019.
- [61] Basava Naga Girish Koneru and Vinita Vasudevan. Sparse artificial neural networks using a novel smoothed lasso penalization. *IEEE Transactions on Circuits and Systems II: Express Briefs*, 66(5):848–852, 2019.
- [62] H. Sahbi, P. Etyngier, J-Y. Audibert, R. Keriven. Manifold learning using robust graph laplacian for interactive image search. 2008 IEEE Conference on Computer Vision and Pattern Recognition, 1-8
- [63] Alex Krizhevsky, Ilya Sutskever, and Geoffrey E Hinton. Imagenet classification with deep convolutional neural networks. *Communications of the ACM*, 60(6):84–90, 2017.
- [64] Yann LeCun, John Denker, and Sara Solla. Optimal brain damage. *Advances in neural information processing systems*, 2, 1989.
- [65] Inwoong Lee, Doyoung Kim, Seoungyoon Kang, and Sanghoon Lee. Ensemble deep learning for skeleton-based action recognition using temporal sliding lstm networks. In *Proceedings of the IEEE international conference on computer vision*, pages 1012–1020, 2017.
- [66] H. Sahbi, Jean-Yves Audibert, Jaonary Rabarisoa, and Renaud Keriven. "Context-dependent kernel design for object matching and recognition." In 2008 IEEE Conference on Computer Vision and Pattern Recognition, pp. 1-8. IEEE, 2008.
- [67] Carl Lemaire, Andrew Achkar, and Pierre-Marc Jodoin. Structured pruning of neural networks with budget-aware regularization. In *Proceedings of the IEEE/CVF Conference on Computer Vision and Pattern Recognition*, pages 9108–9116, 2019.
- [68] H. Sahbi. "Coarse-to-fine deep kernel networks." IEEE ICCV-W, 2017.
- [69] Ron Levie, Federico Monti, Xavier Bresson, and Michael M Bronstein. Cayleynets: Graph convolutional neural networks with complex rational spectral filters. *IEEE Transactions on Signal Processing*, 67(1):97–109, 2018.
- [70] Bin Li, Xi Li, Zhongfei Zhang, and Fei Wu. Spatio-temporal graph routing for skeleton-based action recognition. In *Proceedings of the AAAI Conference on Artificial Intelligence*, volume 33, pages 8561–8568, 2019.
- [71] M. Jiu and H. Sahbi. "Laplacian deep kernel learning for image annotation." IEEE ICASSP, 2016.
- [72] Chaolong Li, Zhen Cui, Wenming Zheng, Chunyan Xu, and Jian Yang. Spatio-temporal graph convolution for skeleton based action recognition. In *Proceedings of the AAAI conference on artificial intelligence*, volume 32, 2018.
- [73] Hao Li, Asim Kadav, Igor Durdanovic, Hanan Samet, and Hans Peter Graf. Pruning filters for efficient convnets. *arXiv preprint arXiv:1608.08710*, 2016.
- [74] Ruoyu Li, Sheng Wang, Feiyun Zhu, and Junzhou Huang. Adaptive graph convolutional neural networks. In *Proceedings of the AAAI conference on artificial intelligence*, volume 32, 2018.
- [75] N. Bourdis, D. Marraud and H. Sahbi. "Camera pose estimation using visual servoing for aerial video change detection." IEEE IGARSS 2012.
- [76] Sheng Li, Tingting Jiang, Tiejun Huang, and Yonghong Tian. Global co-occurrence feature learning and active coordinate system conversion for skeleton-based action recognition. In *Proceedings of the IEEE/CVF winter conference on applications of computer vision*, pages 586–594, 2020.
- [77] Wenbo Li, Longyin Wen, Mooi Choo Chuah, and Siwei Lyu. Category-blind human action recognition: A practical recognition system. In *Proceedings of the IEEE international conference on computer vision*, pages 4444–4452, 2015.
- [78] H. Sahbi and N. Boujemaa. "Robust matching by dynamic space warping for accurate face recognition." Proceedings 2001 International Conference on Image Processing (Cat. No. 01CH37205). Vol. 1. IEEE, 2001.
- [79] Jianbo Liu, Yongcheng Liu, Ying Wang, Veronique Prinnet, Shiming Xiang, and Chunhong Pan. Decoupled representation learning for skeleton-based gesture recognition. In *Proceedings of the IEEE/CVF Conference on Computer Vision and Pattern Recognition*, pages 5751–5760, 2020.
- [80] Jianbo Liu, Ying Wang, Shiming Xiang, and Chunhong Pan. Han: An efficient hierarchical self-attention network for skeleton-based gesture recognition. *arXiv preprint arXiv:2106.13391*, 2021.
- [81] Sabrina Tollari, Philippe Mulhem, Marin Ferecatu, Hervé Glotin, Marcin Detyniecki, Patrick Gallinari, H. Sahbi, and Zhong-Qiu Zhao. "A comparative study of diversity methods for hybrid text and image retrieval approaches." In Workshop of the Cross-Language Evaluation Forum for European Languages, pp. 585-592. Springer, Berlin, Heidelberg, 2008.
- [82] Jun Liu, Amir Shahroudy, Dong Xu, and Gang Wang. Spatio-temporal lstm with trust gates for 3d human action recognition. In *Computer Vision—ECCV 2016: 14th European Conference, Amsterdam, The Netherlands, October 11-14, 2016, Proceedings, Part III 14*, pages 816–833. Springer, 2016.
- [83] Jun Liu, Gang Wang, Ling-Yu Duan, Kamila Abdiyeva, and Alex C Kot. Skeleton-based human action recognition with global context-aware attention lstm networks. *IEEE Transactions on Image Processing*, 27(4):1586–1599, 2017.

- [84] Q. Oliveau and H. Sahbi. "Learning attribute representations for remote sensing ship category classification." *IEEE JSTARS* 10.6 (2017): 2830-2840.
- [85] Jun Liu, Gang Wang, Ping Hu, Ling-Yu Duan, and Alex C Kot. Global context-aware attention lstm networks for 3d action recognition. In *Proceedings of the IEEE conference on computer vision and pattern recognition*, pages 1647-1656, 2017.
- [86] Mengyuan Liu, Hong Liu, and Chen Chen. Enhanced skeleton visualization for view invariant human action recognition. *Pattern Recognition*, 68:346-362, 2017.
- [87] H. Sahbi. "Interactive satellite image change detection with context-aware canonical correlation analysis." *IEEE GRSL*, (14)5, 2017.
- [88] Mengyuan Liu and Junsong Yuan. Recognizing human actions as the evolution of pose estimation maps. In *Proceedings of the IEEE Conference on Computer Vision and Pattern Recognition*, pages 1159-1168, 2018.
- [89] Zhuang Liu, Jianguo Li, Zhiqiang Shen, Gao Huang, Shoumeng Yan, and Changshui Zhang. Learning efficient convolutional networks through network slimming. In *Proceedings of the IEEE international conference on computer vision*, pages 2736-2744, 2017.
- [90] Christos Louizos, Max Welling, and Diederik P Kingma. Learning sparse neural networks through l_0 regularization. *arXiv preprint arXiv:1712.01312*, 2017.
- [91] H. Sahbi. "Relevance feedback for satellite image change detection." *IEEE ICASSP*, 2013.
- [92] Mehran Maghoubi and Joseph J LaViola. Deepgru: Deep gesture recognition utility. In *Advances in Visual Computing: 14th International Symposium on Visual Computing, ISVC 2019, Lake Tahoe, NV, USA, October 7-9, 2019, Proceedings, Part I 14*, pages 16-31. Springer, 2019.
- [93] Ahmed Mazari and Hichem Sahbi. Deep temporal pyramid design for action recognition. In *IEEE International Conference on Acoustics, Speech and Signal Processing (ICASSP)*, pages 2077-2081. IEEE, 2019.
- [94] Ahmed Mazari and Hichem Sahbi. Mlgn: Multi-laplacian graph convolutional networks for human action recognition. In *The British Machine Vision Conference (BMVC)*, 2019.
- [95] Moustafa Meshry, Mohamed E Hussein, and Marwan Torki. Linear-time online action detection from 3d skeletal data using bags of gesturelets. In *2016 IEEE winter conference on applications of computer vision (WACV)*, pages 1-9. IEEE, 2016.
- [96] Alessio Micheli. Neural network for graphs: A contextual constructive approach. *IEEE Transactions on Neural Networks*, 20(3):498-511, 2009.
- [97] Seyed Iman Mirzadeh, Mehrdad Farajtabar, Ang Li, Nir Levine, Akihiro Matsukawa, and Hassan Ghasemzadeh. Improved knowledge distillation via teacher assistant. In *Proceedings of the AAAI conference on artificial intelligence*, volume 34, pages 5191-5198, 2020.
- [98] Xuan Son Nguyen, Luc Brun, Olivier Lézoray, and Sébastien Bougleux. A neural network based on spd manifold learning for skeleton-based hand gesture recognition. In *Proceedings of the IEEE/CVF Conference on Computer Vision and Pattern Recognition*, pages 12036-12045, 2019.
- [99] N. Bourdis, D. Marraud and H. Sahbi. "Constrained optical flow for aerial image change detection." in *IEEE IGARSS*, 2011.
- [100] Juan C Nunez, Raul Cabido, Juan J Pantrigo, Antonio S Montemayor, and Jose F Velez. Convolutional neural networks and long short-term memory for skeleton-based human activity and hand gesture recognition. *Pattern Recognition*, 76:80-94, 2018.
- [101] Juan C Nunez, Raul Cabido, Juan J Pantrigo, Antonio S Montemayor, and Jose F Velez. Convolutional neural networks and long short-term memory for skeleton-based human activity and hand gesture recognition. *Pattern Recognition*, 76:80-94, 2018.
- [102] N. Bourdis, D. Marraud, and H. Sahbi, Spatio-temporal interaction for aerial video change detection, in *IGARSS*, 2012, pp. 2253-2256
- [103] Eshed Ohn-Bar and Mohan Manubhai Trivedi. Hand gesture recognition in real time for automotive interfaces: A multimodal vision-based approach and evaluations. *IEEE transactions on intelligent transportation systems*, 15(6):2368-2377, 2014.
- [104] Hichem Sahbi. Kernel-based graph convolutional networks. In *25th International Conference on Pattern Recognition (ICPR)*, pages 4887-4894. IEEE, 2021.
- [105] Omar Oreifej and Zicheng Liu. Hon4d: Histogram of oriented 4d normals for activity recognition from depth sequences. In *Proceedings of the IEEE conference on computer vision and pattern recognition*, pages 716-723, 2013.
- [106] Wei Pan, Hao Dong, and Yike Guo. Dropneuron: Simplifying the structure of deep neural networks. *arXiv preprint arXiv:1606.07326*, 2016.
- [107] Hichem Sahbi. Learning connectivity with graph convolutional networks. In *25th International Conference on Pattern Recognition (ICPR)*, pages 9996-10003. IEEE, 2021.
- [108] H. Wannous Q. De Smedt and J.-P. Vandeborre. Skeleton-based dynamic hand gesture recognition. *Proc. IEEE Comput. Soc. Conf. Comput. Vis. Pattern Recognit. Workshops (CVPRW), Las Vegas, NV, United states, june, pp 1206-1214*, 2016.
- [109] Hossein Rahmani and Ajmal Mian. 3d action recognition from novel viewpoints. In *Proceedings of the IEEE Conference on Computer Vision and Pattern Recognition*, pages 1506-1515, 2016.
- [110] Olaf Ronneberger, Philipp Fischer, and Thomas Brox. U-net: Convolutional networks for biomedical image segmentation. In *Medical Image Computing and Computer-Assisted Intervention-MICCAI 2015: 18th International Conference, Munich, Germany, October 5-9, 2015, Proceedings, Part III 18*, pages 234-241. Springer, 2015.

- [111] Hichem Sahbi. Kernel pca for similarity invariant shape recognition. *Neurocomputing*, 70(16-18):3034–3045, 2007.
- [112] Mark Sandler, Andrew Howard, Menglong Zhu, Andrey Zhmoginov, and Liang-Chieh Chen. Mobilenetv2: Inverted residuals and linear bottlenecks. In *Proceedings of the IEEE conference on computer vision and pattern recognition*, pages 4510–4520, 2018.
- [113] Amir Shahroudy, Jun Liu, Tian-Tsong Ng, and Gang Wang. Ntu rgb+ d: A large scale dataset for 3d human activity analysis. In *Proceedings of the IEEE conference on computer vision and pattern recognition*, pages 1010–1019, 2016.
- [114] Hichem Sahbi. Learning laplacians in chebyshev graph convolutional networks. In *Proceedings of the IEEE/CVF International Conference on Computer Vision*, pages 2064–2075, 2021.
- [115] Lei Shi, Yifan Zhang, Jian Cheng, and Hanqing Lu. Non-local graph convolutional networks for skeleton-based action recognition. *arXiv preprint arXiv:1805.07694*, 1(2):3, 2018.
- [116] Sijie Song, Cuiling Lan, Junliang Xing, Wenjun Zeng, and Jiaying Liu. An end-to-end spatio-temporal attention model for human action recognition from skeleton data. In *Proceedings of the AAAI conference on artificial intelligence*, volume 31, 2017.
- [117] Mingxing Tan and Quoc Le. Efficientnet: Rethinking model scaling for convolutional neural networks. In *International conference on machine learning*, pages 6105–6114. PMLR, 2019.
- [118] Hichem Sahbi. Lightweight connectivity in graph convolutional networks for skeleton-based recognition. In *IEEE International Conference on Image Processing (ICIP)*, pages 2329–2333. IEEE, 2021.
- [119] Raviteja Vemulapalli, Felipe Arrate, and Rama Chellappa. Human action recognition by representing 3d skeletons as points in a lie group. In *Proceedings of the IEEE conference on computer vision and pattern recognition*, pages 588–595, 2014.
- [120] Li Wan, Matthew Zeiler, Sixin Zhang, Yann Le Cun, and Rob Fergus. Regularization of neural networks using dropout. In *International conference on machine learning*, pages 1058–1066. PMLR, 2013.
- [121] Hongsong Wang and Liang Wang. Modeling temporal dynamics and spatial configurations of actions using two-stream recurrent neural networks. In *Proceedings of the IEEE conference on computer vision and pattern recognition*, pages 499–508, 2017.
- [122] Ling Wang and Hichem Sahbi. Directed acyclic graph kernels for action recognition. In *Proceedings of the IEEE International Conference on Computer Vision*, pages 3168–3175, 2013.
- [123] Ling Wang and Hichem Sahbi. Bags-of-daglets for action recognition. In *IEEE International Conference on Image Processing (ICIP)*, pages 1550–1554. IEEE, 2014.
- [124] Pichao Wang, Wanqing Li, Zhimin Gao, Jing Zhang, Chang Tang, and Philip O Ogunbona. Action recognition from depth maps using deep convolutional neural networks. *IEEE Transactions on Human-Machine Systems*, 46(4):498–509, 2015.
- [125] Pichao Wang, Wanqing Li, Philip Ogunbona, Jun Wan, and Sergio Escalera. Rgb-d-based human motion recognition with deep learning: A survey. *Computer Vision and Image Understanding*, 171:118–139, 2018.
- [126] Hichem Sahbi. Topologically-consistent magnitude pruning for very lightweight graph convolutional networks. In *IEEE International Conference on Image Processing (ICIP)*, pages 3495–3499. IEEE, 2022.
- [127] Pichao Wang, Zhaoyang Li, Yonghong Hou, and Wanqing Li. Action recognition based on joint trajectory maps using convolutional neural networks. In *Proceedings of the 24th ACM international conference on Multimedia*, pages 102–106, 2016.
- [128] Wei Wen, Chunpeng Wu, Yandan Wang, Yiran Chen, and Hai Li. Learning structured sparsity in deep neural networks. *Advances in neural information processing systems*, 29, 2016.
- [129] Yu-Hui Wen, Lin Gao, Hongbo Fu, Fang-Lue Zhang, and Shihong Xia. Graph cnns with motif and variable temporal block for skeleton-based action recognition. In *Proceedings of the AAAI conference on artificial intelligence*, volume 33, pages 8989–8996, 2019.
- [130] Hichem Sahbi. Phase-field models for lightweight graph convolutional networks. In *Proceedings of the IEEE/CVF Conference on Computer Vision and Pattern Recognition*, pages 4643–4649, 2023.
- [131] Junwu Weng, Mengyuan Liu, Xudong Jiang, and Junsong Yuan. Deformable pose traversal convolution for 3d action and gesture recognition. In *Proceedings of the European conference on computer vision (ECCV)*, pages 136–152, 2018.
- [132] Simon Wiedemann, Arturo Marban, Klaus-Robert Müller, and Wojciech Samek. Entropy-constrained training of deep neural networks. In *2019 International Joint Conference on Neural Networks (IJCNN)*, pages 1–8. IEEE, 2019.
- [133] Hichem Sahbi, Jean-Yves Audibert, and Renaud Keriven. Context-dependent kernels for object classification. *IEEE transactions on pattern analysis and machine intelligence*, 33(4):699–708, 2011.
- [134] Zonghan Wu, Shirui Pan, Fengwen Chen, Guodong Long, Chengqi Zhang, and S Yu Philip. A comprehensive survey on graph neural networks. *IEEE transactions on neural networks and learning systems*, 32(1):4–24, 2020.
- [135] Lu Xia, Chia-Chih Chen, and Jake K Aggarwal. View invariant human action recognition using histograms of 3d joints. In *2012 IEEE computer society conference on computer vision and pattern recognition workshops*, pages 20–27. IEEE, 2012.
- [136] Sijie Yan, Yuanjun Xiong, and Dahua Lin. Spatial temporal graph convolutional networks for skeleton-based action recognition. In *Proceedings of the AAAI conference on artificial intelligence*, volume 32, 2018.
- [137] Hichem Sahbi and François Fleuret. Kernel methods and scale invariance using the triangular kernel. Technical report, INRIA, 2004.
- [138] Xiaodong Yang and YingLi Tian. Effective 3d action recognition using eigenjoints. *Journal of Visual Communication and Image Representation*, 25(1):2–11, 2014.
- [139] Fei Yuan, Gui-Song Xia, Hichem Sahbi, and Veronique Prinet. Mid-level features and spatio-temporal context for activity recognition. *Pattern Recognition*, 45(12):4182–4191, 2012.

- [140] Kiwon Yun, Jean Honorio, Debaleena Chattopadhyay, Tamara L Berg, and Dimitris Samaras. Two-person interaction detection using body-pose features and multiple instance learning. In *2012 IEEE computer society conference on computer vision and pattern recognition workshops*, pages 28–35. IEEE, 2012.
- [141] Mihai Zanfir, Marius Leordeanu, and Cristian Sminchisescu. The moving pose: An efficient 3d kinematics descriptor for low-latency action recognition and detection. In *Proceedings of the IEEE international conference on computer vision*, pages 2752–2759, 2013.
- [142] Hichem Sahbi and Donald Geman. A hierarchy of support vector machines for pattern detection. *Journal of Machine Learning Research*, 7(10), 2006.
- [143] Pengfei Zhang, Cuiling Lan, Junliang Xing, Wenjun Zeng, Jianru Xue, and Nanning Zheng. View adaptive recurrent neural networks for high performance human action recognition from skeleton data. In *Proceedings of the IEEE international conference on computer vision*, pages 2117–2126, 2017.
- [144] Songyang Zhang, Xiaoming Liu, and Jun Xiao. On geometric features for skeleton-based action recognition using multilayer lstm networks. In *2017 IEEE Winter Conference on Applications of Computer Vision (WACV)*, pages 148–157. IEEE, 2017.
- [145] Mingyuan Jiu and Hichem Sahbi. Nonlinear deep kernel learning for image annotation. *IEEE Transactions on Image Processing*, 26(4):1820–1832, 2017.
- [146] Xikang Zhang, Yin Wang, Mengran Gou, Mario Sznaier, and Octavia Camps. Efficient temporal sequence comparison and classification using gram matrix embeddings on a riemannian manifold. In *Proceedings of the IEEE conference on computer vision and pattern recognition*, pages 4498–4507, 2016.
- [147] Ying Zhang, Tao Xiang, Timothy M Hospedales, and Huchuan Lu. Deep mutual learning. In *Proceedings of the IEEE conference on computer vision and pattern recognition*, pages 4320–4328, 2018.
- [148] Ziwei Zhang, Peng Cui, and Wenwu Zhu. Deep learning on graphs: A survey. *IEEE Transactions on Knowledge and Data Engineering*, 34(1):249–270, 2020.
- [149] Wentao Zhu, Cuiling Lan, Junliang Xing, Wenjun Zeng, Yanghao Li, Li Shen, and Xiaohui Xie. Co-occurrence feature learning for skeleton based action recognition using regularized deep lstm networks. In *Proceedings of the AAAI conference on artificial intelligence*, volume 30, 2016.
- [150] P. Vo and H. Sahbi. “Transductive kernel map learning and its application to image annotation.” *BMVC*. 2012.